

# Measurement of the full excitation spectrum of the ${}^7\text{Li}(p,\gamma)\alpha\alpha$ reaction at 441 keV

Michael Munch, Oliver Sølund Kirsebom, Jacobus Andreas Swartz, Karsten Riisager, Hans Otto Uldall Fynbo

*Department of Physics and Astronomy, Aarhus University, Denmark*

## Abstract

A current challenge for *ab initio* calculations is systems that contain large continuum contributions such as  ${}^8\text{Be}$ . We report on new measurements of radiative decay widths in this nucleus that test recent Green's function Monte Carlo calculations.

Traditionally,  $\gamma$  ray detectors have been utilized to measure the high energy photons from the  ${}^7\text{Li}(p,\gamma)\alpha\alpha$  reaction. However, due to the complicated response function of these detectors it has not yet been possible to extract the full  $\gamma$  ray spectrum from this reaction. Here we present an alternative measurement using large area Silicon detectors to detect the two  $\alpha$  particles, which provides a practically background free spectrum and retains good energy resolution.

The resulting spectrum is analyzed using a many-level multi channel R-matrix parametrization. Improved values for the radiative widths are extracted from the R-matrix fit. We find evidence for significant non-resonant continuum contributions and tentative evidence for a broad  $0^+$  resonance at 12 MeV.

**Keywords:** *ab initio*, R-matrix,  ${}^8\text{Be}$ , radiative decay width, light nuclei

## 1. Introduction

In recent years *ab initio* calculations of atomic nuclei, such as Green's function Monte Carlo (GFMC) [1] and No Core Shell Model (NCSM) [2], have advanced tremendously and now provide quite accurate predictions for light nuclei. Historically, NCSM has struggled with highly clustered states. However, the method has recently been combined with the resonating group method (RGM) to better describe clustered nuclei including continuum properties [2].

In this context  ${}^8\text{Be}$  provides an interesting benchmark. All states in this isotope are unbound with its ground state located just 92 keV above the  $2\alpha$  threshold. The lowest two states are highly clustered while some of the resonances at higher energy couple relatively weakly to the  $2\alpha$  final state.

GFMC calculations of electromagnetic transitions in  ${}^8\text{Be}$  have been performed by Pastore *et al.* [1], and experimentally  $\gamma$  decays of several states in  ${}^8\text{Be}$  have been measured. The focus of the present letter is the  $\gamma$  decay of the 17.64 MeV  $1^+$  state. M1 decays of this state could populate both  $0^+$  and  $2^+$  states. There are two measurements of the transition strength to the ground- and first excited states in  ${}^8\text{Be}$  [3, 4], and two measurements of transitions to the  $2^+$  doublet at 16.6-16.9 MeV [5, 6]. However, due to the complicated response function of previous measurements it has not been possible to extract the full  $\gamma$  ray spectrum - specifically none of the previous measurements

were sensitive to  $\gamma$  decays into the unresolved energy region below the  $2^+$  doublet.

This region was resolved experimentally using e.g.  $\alpha$ - $\alpha$  scattering and the  $\beta$ -decay of  ${}^8\text{B}$  and  ${}^8\text{Li}$  [7]. To understand these different ways of populating  ${}^8\text{Be}$ , it is necessary to have contributions not only from the known resonances, but also a broad contribution [7] between the first excited state at 3 MeV and the isospin mixed  $2^+$  doublet at 16.6-16.9 MeV. It is unclear if this contribution represents a  $2^+$  intruder state, a non-resonant continuum contribution, or the low energy tails of high energy resonances [7, 8]. From theory there is also a prediction of a  $0^+$  T=0 intruder state at around 12 MeV [9].

In this letter we will present a measurement of the  $\gamma$  decay of the 17.64 MeV  $1^+$  state using a method which is sensitive to this region of interest and essentially background free. By this method we will not only address the question of intruder states, but also derive new more reliable values for the partial decay widths of the already measured transitions.

It should be noted that electromagnetic transitions from the  $1^+$  states of  ${}^8\text{Be}$  are also of high current interest due to the observation of anomalous internal pair creation in  ${}^8\text{Be}$  and the interpretation of that as a possible indication of a new light, neutral boson [10, 11].

## 2. Experiment

The experiment was conducted at the 5MV Van de Graaff accelerator at Aarhus University that provided a beam of  $\text{H}_3^+$  with energies between 1305 keV and 1410 keV.

\*Corresponding author

Email address: [munch@phys.au.dk](mailto:munch@phys.au.dk) (Michael Munch)

The 17.64 MeV state was populated using the  ${}^7\text{Li}(p,\gamma)$  reaction as illustrated on Fig. 1. The beam current was measured using a suppressed Faraday cup 1 m downstream of the target. Typical beam currents were between 200 pA and 1 nA and the beam spot was defined by a pair of  $1 \times 1$  mm vertical and horizontal slits. The beam impinged on a natural LiF target manufactured in house by evaporation of a 160 nm ( $\pm 10\%$ ) layer of natural lithium fluoride onto a thin  $\sim 4 \mu\text{g cm}^{-2}$  carbon backing.

The 17.64 MeV state was populated resonantly via  ${}^7\text{Li}(p,\gamma)$  as depicted in Fig. 1. While gamma rays were not directly observed, the occurrence of electromagnetic de-excitation was inferred indirectly from the energies of the two  $\alpha$  particles emitted in the subsequent breakup. Charged particles were detected with two double-sided silicon strip detectors (DSSD) of the W1 type from Micron Semiconductors [12] giving a simultaneous measurement of position and energy. Each detector had an active area of  $5 \times 5$  cm divided into  $16 \times 16$  orthogonal strips and was positioned 4 cm from the target at 90 deg with respect to the beam axis.

A resonance scan was performed with proton energies from 435 to 470 keV and afterwards data was acquired at 446 keV for 52 hours and at 455 keV for 63 hours.

### 3. Data reduction

The data was analyzed using the full kinematic approach as described in Ref. [13]. The signal of interest is two coincident  $\alpha$  particles with missing energy corresponding to the reaction  $p + {}^7\text{Li} \rightarrow {}^8\text{Be}^* \rightarrow \gamma + \alpha + \alpha$  as illustrated in Fig. 1.

Our coincidence requirement is a time difference of less than 13 ns. As our coincidence timing resolution is 9.3 ns FWHM this includes  $> 99\%$  of all true coincidences. All coincidences surviving this cut are then corrected for energy loss in the detector dead-layer and target foil assuming they were  $\alpha$  particles. The energy of each particle in the center of mass (CM) of  $p + {}^7\text{Li}$  reaction was determined from its direction and energy. With a simultaneous detection of two  $\alpha$  particles one can infer the corresponding  ${}^8\text{Be}$

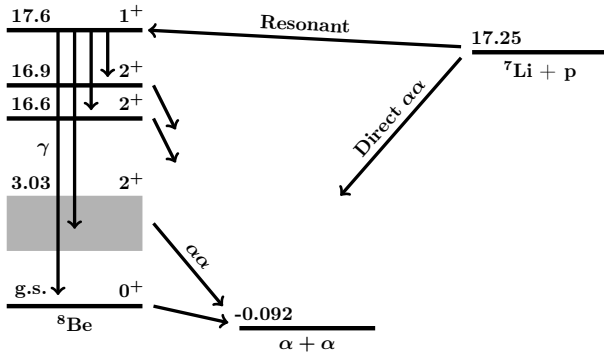


**Figure 1:** Decay scheme. Only levels populated in the  $p + {}^7\text{Li}$  reaction or the  $\gamma$  subsequent decay is shown. Energies are in MeV relative to the  ${}^8\text{Be}$  ground state.

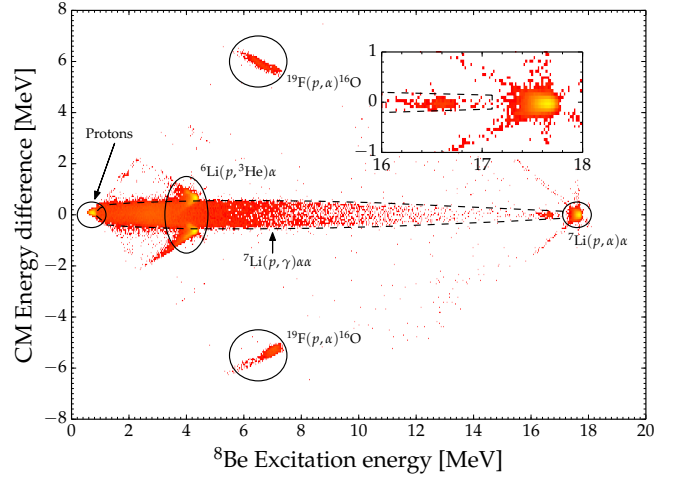


**Figure 2:** Difference in CM energy vs  ${}^8\text{Be}$  excitation energy. The circles mark various background reactions while the band within the dashed contour stretching from 1 to 17 MeV corresponds to  $\gamma$  delayed  $\alpha$  particles. The insert shows the high excitation energy region. The color scale is logarithmic.

excitation energy from their summed 4-momentum. Figure 2 shows the difference in CM energy versus the  ${}^8\text{Be}$  excitation energy. In the limit of zero recoil, conservation of energy and momentum dictates that the two alpha particles should have equal CM energies. When the small, but finite, recoil is taken into account, the CM energy-difference distribution remains centered very close to zero, but acquires a sizable spread. Hence the horizontal band in the figure corresponds to the  ${}^7\text{Li}(p,\gamma)\alpha\alpha$  reaction. At high excitation energy there is a distinct peak corresponding to the direct reaction  ${}^7\text{Li}(p,\alpha)\alpha$ . The two weak diagonal bands extending from the peak correspond to events with insufficient energy loss correction. These do not interfere with the region of interest and their strength is negligible compared to the peak. There are two similar peaks at roughly 4 MeV, which both correspond to  ${}^6\text{Li}(p,\alpha){}^3\text{He}$ . At 7 MeV there are two bands with large deviations from equal energy. This is a background reaction on fluorine  ${}^{19}\text{F}(p,\alpha){}^{16}\text{O}$ . At low energy we see random coincidences with the beam. The identity of the various components was verified with a Monte Carlo simulation. The  $\alpha$ -source energy calibration of the excitation spectrum was cross checked against the  ${}^6\text{Li}(p,\alpha){}^3\text{He}$  and  ${}^7\text{Li}(p,\alpha)\alpha$  peaks and was found to agree within 4 keV with the tabulated values [8]. It should be stressed that this spectrum is essentially background free in the region of interest, except for the small region around the  ${}^6\text{Li}(p,\alpha){}^3\text{He}$  peaks, which will be excluded from the further analysis.

In order to completely remove random coincidences with the beam we require the angle between a pair to be  $> 170^\circ$  and place a low energy cut at 1 MeV. These cuts preserve 99% of the good events. The events corresponding to  $\gamma$  delayed  $\alpha$  emission are selected as those within the dashed contour seen on Fig. 2.

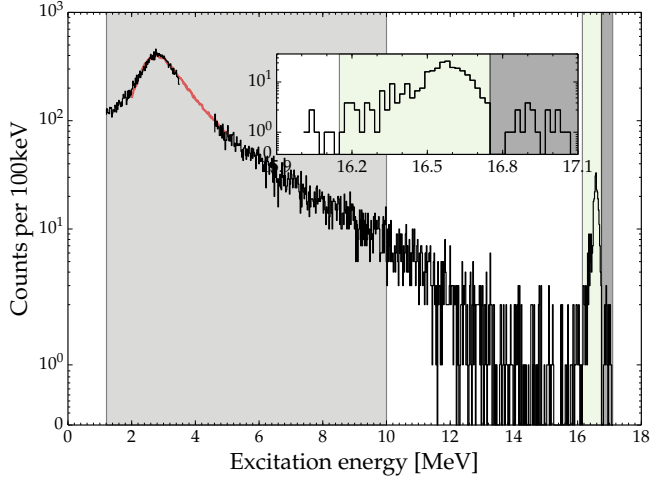


**Figure 3:** Projected excitation spectrum. The superimposed curve is the best fit to the peak of first excited state with a single level R-matrix formula. See Section 4.1 for details.

Figure 3 shows the projected excitation spectrum with the first excited state visible at 3 MeV and the two contributions from the doublet at high energy in the insert. The superimposed curve will be discussed in Section 4.1. The extracted excitation spectrum can be found in [14].

### 3.1. Normalization

Figure 4 shows the yield of events with an excitation energy between 2 and 3 MeV. The red crosses and green triangles correspond to the two long measurements. The solid line shows the best fit to equation 14 from Ref. [15].

$$Y = \left[ \tan^{-1} \frac{E_p - E_r}{\Gamma_{\text{lab}}/2} - \tan^{-1} \frac{E_p - E_r - \Delta E}{\Gamma_{\text{lab}}/2} \right] \times \frac{2\pi}{k_r^2} \frac{g_J}{\epsilon} \Gamma_\gamma, \quad (1)$$

where  $\Gamma_{\text{lab}}$  is the resonance width in the lab system,  $E_p$  is the beam energy,  $E_r$  the resonance energy,  $\Delta E$  the energy loss through the target,  $g_J$  the statistical factor from spin coupling,  $k_r$  the  ${}^7\text{Li}$ -p wave number at the resonance energy, and  $\epsilon = \frac{1}{N} \frac{dE}{dx}$ , where  $N$  is the number density of target nuclei and  $\frac{dE}{dx}$  the stopping power.

$\Gamma_{\text{lab}}$  was fixed to 8/7 of the literature value of 10.7(5) keV [8]. The last part of the equation was treated as a scaling constant and fitted. The best fit was achieved with  $\Delta E = 18.1(16)$  keV and  $E_r = 444.3(6)$  keV. The resonance energy is slightly higher than the latest literature value of 441.4(5) keV [8].

Upon impinging on the target foil the  $\text{H}_3^+$  molecule will break up. In this process additional electron stripping, neutralization and scattering outside the Faraday cup might occur. The effect of these processes can be determined by measuring the integrated current with and without target foil placed in the beam. The ratio of these two measurements gives the effective charge state of the

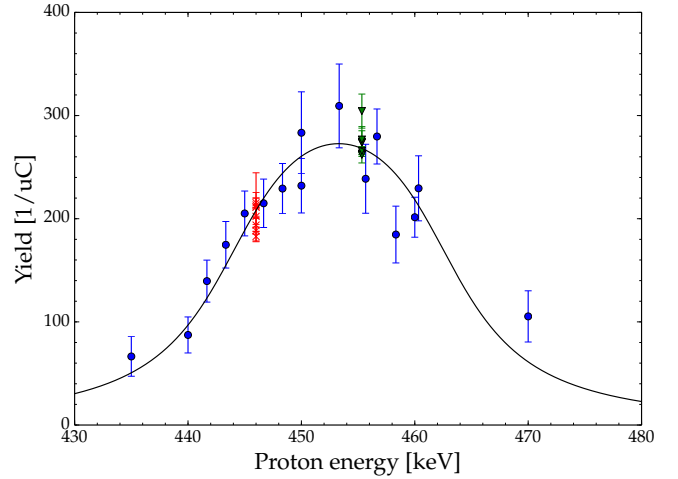


**Figure 4:** Resonance scan showing the yield of events with an excitation energy between 2 and 3 MeV as a function of beam energy. The red crosses and green triangles correspond to the long measurements. Each datapoint corresponds to a run and thus slightly different accelerator settings. The curve is the best fit to Eq. (1) - see text for details.

$\text{H}_3^+$  molecule as observed at the Faraday cup, when the beam passes through the foil. The result was  $2.50(7)e$  over the measured energy range.

## 4. Extraction of radiative widths

As previous experiments have determined the widths using simple integration of the excitation spectrum, we will first determine the widths using this method. In addition, we will perform an R-matrix analysis of the measured spectrum in order to take interference into account. The R-matrix parametrization is described elsewhere [16]. The R-matrix implementation can be found in Ref. [17].

### 4.1. Bin integration

The excitation spectrum, shown in Fig. 3, has been subdivided into four regions covering the first excited state from 1 to 10 MeV, the continuum from 10 to 16.1 MeV and the two doublet states from 16.1 to 16.75 MeV and 16.75 to 17.1 MeV respectively. The choice of 10 MeV is somewhat arbitrary. It is placed sufficiently high to include the majority of the peak. Superimposed on the data is the

**Table 1:** Widths extracted from bin integration of the excitation spectra. Literature values are from Ref. [8]. The GFMC results are from Ref. [1]. The R-matrix results are from Section 4.2.  $\Gamma_{01}$  of the R-matrix results is from model 2, while the rest is from model 3.

Parameter	Present	Lit.	GFMC	R-Mat.
$\Gamma_{01}$ (eV)	-	15.0(18)	12.0(3)	13.8(4)
$\Gamma_{21}$ (eV)	6.0(3)	6.7(13)	3.8(2)	5.01(11)
$\Gamma_{22}$ (meV)	35(3)	32(3)	29.7(3)	38(2)
$\Gamma_{23}$ (meV)	2.1(6)	1.3(3)	2.20(5)	1.6(5)

best fit between 2 and 6 MeV to a single level R-matrix expression fed by an M1 decay.

The widths were determined by integration of the three regions with solid shading. The contribution from the excluded region was determined from the superimposed R-matrix curve. The integrals were converted into absolute decay widths using Eq. (1) and the parameters determined in Section 3.1.

The results and statistical errors are listed in Table 1 along with the current literature values from Ref. [8] and the results of GFMC calculations [1].

#### 4.2. R-matrix analysis

We will analyze the excitation spectrum using three different models. Model 1 is a model with one  $0^+$  ground state and three  $2^+$  resonances. All states are fed by M1  $\gamma$  decays while the  $2_1^+$  resonance is also fed by E2 decays. All initial values were taken from Ref. [8]. To ensure convergence the energy of the  $2_3^+$ , as well as the  $\alpha$  widths of the two highest  $2^+$  resonances and the ground state, were fixed. Model 2 adds an additional  $2^+$  level at high energy fed by an M1 transition. All parameters for this additional level were allowed to vary freely. Furthermore, it was no longer necessary to fix  $E_{2_3}$ . Model 3 adds another  $0^+$  state. However, in order to achieve convergence it was necessary to fix the ground state feeding and the position of the  $2^+$  background pole to the values from model 2. The M1 feeding of all  $2^+$  levels were summed coherently while the M1 contribution to the  $0^+$  and the E2 feeding were added incoherently. Model 1 has 8 free parameters, model 2 has 12 and model 3 has 13.

In order to directly compare the experimental spectrum with the spectrum obtained from R-matrix theory, it is necessary to fold the theoretical spectrum with the experimental response function. For this experimental setup the response function is well described as a Gaussian function with an exponential tail - the one tail variant of Ref. [18]. The parameters were determined with a fit to the  ${}^7\text{Li}(p, \alpha)\alpha$  peak as the effect of the response function is most important for the narrow  $2^+$  levels above 16 MeV. The best fit was achieved with  $\mu = 23.5(5)$  keV,  $\sigma = 27.07(15)$  keV and  $\tau = 39.6(2)$  keV.

Figure 5 shows the best fit for all models with a channel radius of 5 fm. The dashed curves show the single level contributions. It should be noted that all models have a weak dependence on the chosen channel radius, as this influences the shape and peak to tail ratio for the  $0^+$  ground state. A channel radius of 5 fm was chosen, as it minimized  $\chi^2$ .

The parameters corresponding to the best fit are listed in Table 2 along with their errors. In order to minimize bias a Poisson likelihood estimator has been used [19]. Errors have been estimated using the MINOS routine and are symmetric unless noted otherwise. Propagated errors have been calculated using the Hessian approximation.

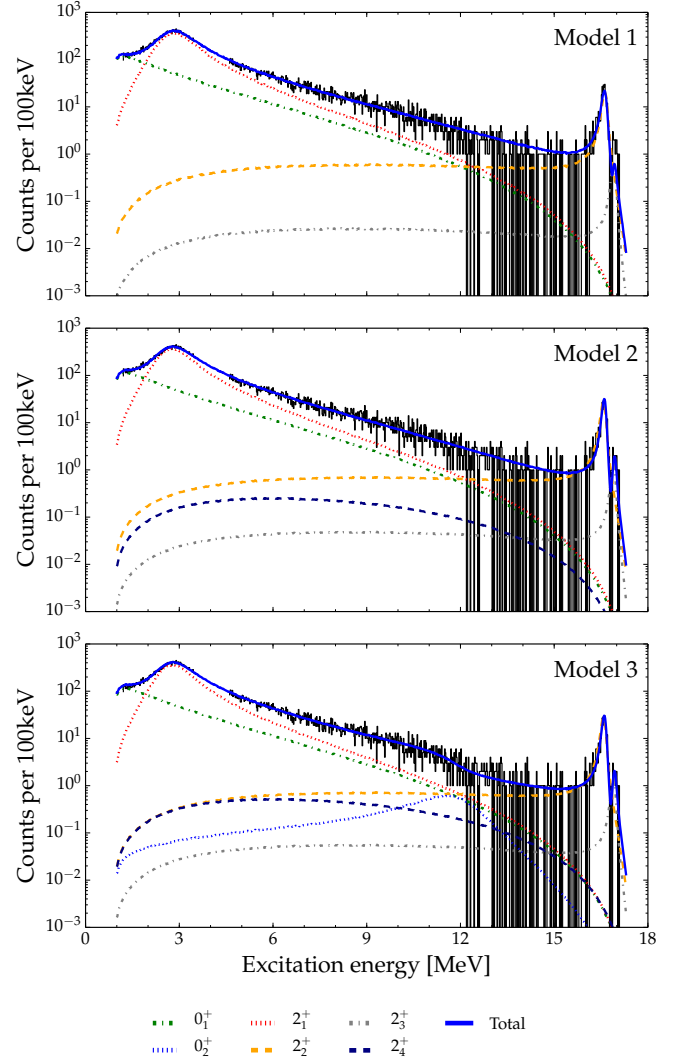


**Figure 5:** Best fit for a channel radius of 5 fm. The solid blue line shows the sum of all contributions, while the dotted shows the single level profile of the individuals levels.

## 5. Discussion

Comparing the radiative widths determined using integration with those from the literature, we find agreement for the doublet. Previous measurements assigned everything below the ground state peak in the  $\gamma$  spectrum to the  $2_1$  distribution. In light of this and considering that our measurement of the  $2_1$  distribution has not been extrapolated to zero energy, the agreement with literature is reasonable.

The excitation spectrum produced by the three R-matrix models can be seen in Fig. 5 and in all cases the majority of the experimental spectrum has been reproduced. The main qualitative improvement between model 1 and 2 is observed around the 16.9 MeV peak, which model 1 systematically undershoots. In addition, an order of magnitude improvement of the P-value is observed for each subsequent model. The single level shape of the model 2

background pole is a broad featureless distribution. We interpret this as non-resonant continuum contributions. An interesting aspect of all models is the significant contribution of the ground state in all energy regions and its dominance below 2 MeV. From this rather remarkable feature it is possible to determine the ground state strength from a measurement well above the peak. This behavior is the well known "ghost anomaly" expected both from theory [20] and observed in previous experiments on the  $^8\text{Be}$  system [21]. This implies that previous measurements, which have ignored the anomaly, have overestimated the  $2_1$  strength by at least 20%. This estimate is based on the

difference between our two different methods.

Additionally, it should be noted that the observed strength in the intermediate region between 6 and 16 MeV cannot be attributed to a single resonance but rather a result of several interfering levels and non-resonant continuum contributions. The extracted  $\gamma$  widths for the three models agree within the statistical errors except for the  $2_2$  width. However, as model 1 systematically deviates in that region we recommend that the model 3 parameters are used. The change in resonance energy is expected from interference and similar effects were observed in  $\beta$  decay experiments [22].

**Table 2:** Parameters for the best fit for both models with a channel radius of 5 fm. Parameters in square brackets were fixed. Decay widths were calculated with eq. (6) from the supplementary information. All errors are statistical. Propagated errors are calculated using the Hessian approximation.

Parameter	Model 1	Model 2	Model 3
$E_{0_1}$ (keV)	[0]	[0]	[0]
$\gamma_{0_1 M1}$ ( $10^{-11} \times \text{eV}^{-1}$ )	$4.35 \pm 0.05$	$4.36 \pm 0.06$	[4.36]
$\Gamma_{0_1 M1}^0$ (eV)	$13.7 \pm 0.3$	$13.8 \pm 0.4$	[13.8]
$\gamma_{0_1 \alpha_0}$ ( $\sqrt{\text{keV}}$ )	[22.1]	[22.1]	[22.1]
$\Gamma_{0_1 \alpha_0}^0$ (eV)	[5.57]	[5.57]	[5.57]
$E_{0_2}$ (MeV)	-	-	$12.0 \pm 0.3$
$\gamma_{0_2 M1}$ ( $10^{-11} \times \text{eV}^{-1}$ )	-	-	$0.58 \pm 0.08$
$\Gamma_{0_2 M1}^0$ (eV)	-	-	$12 \pm 3$
$\gamma_{0_2 \alpha_0}$ ( $\sqrt{\text{keV}}$ )	-	-	$-15.2 \pm 1.5$
$\Gamma_{0_2 \alpha_0}^0$ (MeV)	-	-	$2.4 \pm 0.5$
$E_{2_1}$ (keV)	$3008^{+55}_{-9}$	$2960 \pm 22$	$2969 \pm 11$
$\gamma_{2_1, M1}$ ( $10^{-11} \times \text{eV}^{-1}$ )	$3.31 \pm 0.03$	$3.22 \pm 0.06$	$3.13 \pm 0.03$
$\Gamma_{2_1, M1}^0$ (eV)	$5.57 \pm 0.11$	$5.3 \pm 0.2$	$5.01 \pm 0.11$
$\gamma_{2_1, E2}$ ( $10^{-22} \times \text{eV}^{-3}$ )	$-4.2 \pm 1.2$	$-4 \pm 500$	$0.9 \pm 59.2$
$\Gamma_{2_1, E2}^0$ (meV)	$1.9 \pm 1.2$	$< 10 \text{ meV}$	$< 1 \text{ meV}$
$\gamma_{2_1, \alpha_2}$ ( $\sqrt{\text{keV}}$ )	$-29.9^{+0.3}_{-1.5}$	$-29.3 \pm 0.5$	$28.6 \pm 0.3$
$\Gamma_{2_1, \alpha_2}^0$ (MeV)	$1701 \pm 27$	$1601 \pm 45$	$1546 \pm 25$
$E_{2_2}$ (keV)	$16\,629 \pm 11$	$16\,588 \pm 5$	$16\,590 \pm 5$
$\gamma_{2_2, M1}$ ( $10^{-11} \times \text{eV}^{-1}$ )	$11.6 \pm 0.7$	$12.7 \pm 0.4$	$12.9 \pm 0.4$
$\Gamma_{2_2, M1}^0$ (meV)	$27.9 \pm 1.7$	$38 \pm 2$	$38 \pm 2$
$\gamma_{2_2, \alpha_2}$ ( $\sqrt{\text{keV}}$ )	[3.1]	[3.1]	[3.1]
$\Gamma_{2_2, \alpha_2}^0$ (keV)	[108]	[108]	[108]
$E_{2_3}$ (keV)	[16922]	$16\,912 \pm 25$	$16\,910 \pm 23$
$\gamma_{2_3, M1}$ ( $10^{-11} \times \text{eV}^{-1}$ )	$3.2^{+1.7}_{-0.9}$	$4.3 \pm 0.8$	$4.5 \pm 0.7$
$\Gamma_{2_3, M1}^0$ (meV)	$0.8 \pm 0.8$	$1.4 \pm 0.5$	$1.6 \pm 0.5$
$\gamma_{2_3, \alpha_2}$ ( $\sqrt{\text{keV}}$ )	[2.2]	[2.2]	[2.2]
$\Gamma_{2_3, \alpha_2}^0$ (keV)	[74]	[74]	[74]
$E_{2_4}$ (MeV)	-	$24 \pm 3$	[24]
$\gamma_{2_4, M1}$ ( $10^{-11} \times \text{eV}^{-1}$ )	-	$-1.1 \pm 0.2$	$-1.8 \pm 0.2$
$\Gamma_{2_4, M1}^0$ (meV)	-	$57 \pm 20$	$160 \pm 40$
$\gamma_{2_4, \alpha_2}$ ( $\sqrt{\text{keV}}$ )	-	$38 \pm 7$	$35.9 \pm 1.8$
$\Gamma_{2_4, \alpha_2}^0$ (MeV)	-	$20 \pm 8$	$18.0 \pm 1.8$
$\chi^2/\text{ndf}$	878/735	838/731	808/730
$P$ (%)	0.02	0.36	2.3

The second  $0^+$  level, introduced in model 3, interferes destructively with the ground state, as can be observed in the 12 to 16 MeV region where it improves the agreement substantially. Its location is interesting as it coincides precisely with the energy predicted by [9].

The current literature value of 0.12(5) eV in Ref. [8] for the E2 strength is based on the width listed in Table 1 and a measurement of the E2/M1 mixing ratio 0.018(7) [23]. However, all our models yield a significantly smaller ratio  $< 0.002$ . While the errors involved are too large to draw a conclusion, it is important to note that there is significant spread in the reported mixing values [24, 25, 26]. A more detailed measurement of the  $\alpha - \gamma$  correlation function could resolve this issue.

Compared with the GFMC calculation in Ref. [1] we find poor agreement for the transitions to the  $0^+$  and  $2_1^+$  states. For the  $2_1^+$  discrepancy, Ref. [1] suggests that a lack of continuum contributions could explain this. No explanation is given for the  $0^+$  discrepancy. It is interesting to note that a value of  $\Gamma_{2_1 E2} = 0.63(5)$  eV, as suggested by GFMC, can only be accommodated if the first excited state is made extremely wide  $\sim 1.8$  MeV. A similar disagreement is observed for the transitions to the doublet. However, the strength of these transitions depend on isospin mixing of the  $1^+$  doublet states which was first determined by Barker [27]. Using slightly different mixing coefficients resolves some of the issues but create others - see Ref. [1] for details. As these states should be well described in the shell-model, it would be interesting to compare with NCSM calculations of the transition rates.

## 6. Conclusion

Coincident  $\alpha$  particles from the  ${}^7\text{Li}(p, \gamma)\alpha\alpha$  reaction at a proton energy of roughly  $E_p = 441$  keV have been measured using close geometry silicon strip detectors. This yields a background free excitation spectrum from 1 to 17 MeV. The  $\gamma$  decay widths have been determined using both integration and R-matrix analysis.

The results of the R-matrix analysis show that the ground state contributes significantly to the full energy range and dominates the spectrum below 2 MeV. This implies that simply integrating the excitation energy spectrum would overestimate the decay strength to the first excited state. In order to achieve a good fit to data, it is necessary to include a  $2^+$  background pole. This indicates that the spectrum has non-resonant continuum contributions. Additionally, we find tentative evidence for a broad  $0^+$  state at 12 MeV. A similar measurement of the 18.1 MeV  $1^+$  state in  ${}^8\text{Be}$  could further illuminate this.

The extracted widths for the  $2^+$  doublet is in agreement with previous measurements, while the results for the ground and first excited state differ by 8 and 34 % respectively. A comparison with GFMC calculations shows significant differences between 13 and 34 %. Determination of the  $1^+$  isospin mixing might bring clarification.

## 7. Acknowledgement

The authors would like to thank Jonas Refsgaard for his invaluable input on R-matrix theory. Furthermore, we would like to thank Folmer Lyckegaard for manufacturing the target. We also acknowledge financial support from the European Research Council under ERC starting grant LOBENA, No. 307447. OSK acknowledges support from the Villum Foundation.

## References

## References

- [1] S. Pastore, R. B. Wiringa, S. C. Pieper, R. Schiavilla, Quantum Monte Carlo calculations of electromagnetic transitions in Be 8 with meson-exchange currents derived from chiral effective field theory, *Physical Review C* 90 (2) (2014) 024321. doi:10.1103/PhysRevC.90.024321. URL <https://link.aps.org/doi/10.1103/PhysRevC.90.024321>
- [2] S. Baroni, P. Navrátil, S. Quaglioni, Unified ab initio approach to bound and unbound states: No-core shell model with continuum and its application to  ${}^7\text{He}$ , *Physical Review C - Nuclear Physics* 87 (3) (2013) 1–14. arXiv:1301.3450, doi:10.1103/PhysRevC.87.034326.
- [3] W. A. Fowler, C. C. Lauritsen, Gamma-Radiation from Light Nuclei under Proton Bombardment, *Physical Review* 76 (1949) 314.
- [4] D. Zahnow, C. Angulo, C. Rolfs, S. Schmidt, W. H. Schulte, E. Somorjai, The S(E) factor of  ${}^7\text{Li}(p, \gamma){}^8\text{Be}$  and consequences for S(E) extrapolation in  ${}^7\text{Be}(p, \gamma){}^8\text{B}$ , *Zeitschrift für Physik A Hadrons and Nuclei* 351 (2) (1995) 229–236. doi:10.1007/BF01289534. URL <http://adsabs.harvard.edu/abs/1995ZPhyA.351..229Z>
- [5] P. Paul, D. Kohler, K. A. Snover, Magnetic Dipole Transitions and Isospin in Be8, *Physical Review* 173 (4) (1968) 919–930. doi:10.1103/PhysRev.173.919. URL <https://link.aps.org/doi/10.1103/PhysRev.173.919>
- [6] W. E. Sweeney, J. B. Marion, Gamma-Ray Transitions Involving Isobaric-Spin Mixed States in Be 8, *Physical Review* 182 (4) (1969) 1007–1021. doi:10.1103/PhysRev.182.1007. URL <https://link.aps.org/doi/10.1103/PhysRev.182.1007>
- [7] E. K. Warburton, R-matrix analysis of the  $\beta^\pm$ -delayed alpha spectra from the decay of Li8 and B8, *Physical Review C* 33 (1) (1986) 303–313. doi:10.1103/PhysRevC.33.303. URL <https://link.aps.org/doi/10.1103/PhysRevC.33.303>
- [8] D. Tilley, J. Kelley, J. Godwin, D. Millener, J. Purcell, C. Sheu, H. Weller, Energy levels of light nuclei, *Nuclear Physics A* 745 (3-4) (2004) 155–362. doi:10.1016/j.nuclphysa.2004.09.059. URL <http://www.sciencedirect.com/science/article/pii/S0375947404010267><http://linkinghub.elsevier.com/retrieve/pii/S0375947404010267>
- [9] E. Caurier, P. Navrátil, W. E. Ormand, J. P. Vary, Intruder states in  ${}^8\text{Be}$ , *Physical Review C* 64 (5) (2001) 051301. doi:10.1103/PhysRevC.64.051301. URL <https://link.aps.org/doi/10.1103/PhysRevC.64.051301>
- [10] A. J. Krasznahorkay, M. Csatlós, L. Csige, Z. Gács, J. Gulyás, M. Hunyadi, I. Kuti, B. M. Nyakó, L. Stuhl, J. Timár, T. G. Tornyi, Z. Vajta, T. J. Ketel, A. Krasznahorkay, Observation of Anomalous Internal Pair Creation in Be 8 : A Possible Indication of a Light, Neutral Boson, *Physical Review Letters* 116 (4) (2016) 042501. doi:10.1103/PhysRevLett.116.042501. URL <https://link.aps.org/doi/10.1103/PhysRevLett.116.042501>

- [11] J. Kozaczuk, D. E. Morrissey, S. R. Stroberg, Light axial vector bosons, nuclear transitions, and the Be 8 anomaly, *Physical Review D* 95 (11) (2017) 115024. doi:10.1103/PhysRevD.95.115024.  
URL <http://link.aps.org/doi/10.1103/PhysRevD.95.115024>
- [12] O. Tengblad, U. Bergmann, L. Fraile, H. Fynbo, S. Walsh, Novel thin window design for a large-area silicon strip detector, *Nuclear Instruments and Methods in Physics Research Section A: Accelerators, Spectrometers, Detectors and Associated Equipment* 525 (3) (2004) 458–464. doi:10.1016/j.nima.2004.01.082.  
URL <http://linkinghub.elsevier.com/retrieve/pii/S0168900204002414>
- [13] M. Alcorta, O. Kirsebom, M. Borge, H. Fynbo, K. Riisager, O. Tengblad, A complete kinematics approach to study multi-particle final state reactions, *Nuclear Instruments and Methods in Physics Research Section A: Accelerators, Spectrometers, Detectors and Associated Equipment* 605 (3) (2009) 318–325. doi:10.1016/j.nima.2009.03.246.  
URL <http://linkinghub.elsevier.com/retrieve/pii/S0168900209007438>
- [14] M. Munch, O. S. Kirsebom, J. A. Swartz, K. Riisager, H. O. U. Fynbo, 8Be excitation spectrum (Feb. 2018). doi:10.5281/zenodo.1174127.  
URL <https://doi.org/10.5281/zenodo.1174127>
- [15] W. A. Fowler, C. C. Lauritsen, T. Lauritsen, Gamma-Radiation from Excited States of Light Nuclei, *Reviews of Modern Physics* 20 (1) (1948) 236–277. doi:10.1103/RevModPhys.20.236.  
URL <https://link.aps.org/doi/10.1103/RevModPhys.20.236>
- [16] M. Munch, R-Matrix parametrization for  $\gamma$  decays to unbound states [arXiv:1802.09297](https://arxiv.org/abs/1802.09297).  
URL <http://arxiv.org/abs/1802.09297>
- [17] M. Munch, O. S. Kirsebom, J. Refsgaard, Open R-matrix (Feb. 2018). doi:10.5281/zenodo.1174079.  
URL <https://doi.org/10.5281/zenodo.1174079>
- [18] G. Bortels, P. Collaers, Analytical function for fitting peaks in alpha-particle spectra from Si detectors, *International Journal of Radiation Applications and Instrumentation. Part A. Applied Radiation and Isotopes* 38 (10) (1987) 831–837. doi:10.1016/0883-2889(87)90180-8.  
URL <http://linkinghub.elsevier.com/retrieve/pii/0883288987901808>
- [19] U. Bergmann, K. Riisager, A systematic error in maximum likelihood fitting, *Nuclear Instruments and Methods in Physics Research Section A: Accelerators, Spectrometers, Detectors and Associated Equipment* 489 (1-3) (2002) 444–447. doi:10.1016/S0168-9002(02)00864-1.  
URL <http://www.sciencedirect.com/science/article/pii/S0168900202008641>  
<http://linkinghub.elsevier.com/retrieve/pii/S0168900202008641>
- [20] F. C. Barker, P. B. Treacy, Nuclear levels near thresholds, *Nuclear Physics* 38 (1) (1962) 33–49. doi:10.1016/0029-5582(62)91014-3.  
URL [http://www.osti.gov/energycitations/product.biblio.jsp?osti\\_id=4783132](http://www.osti.gov/energycitations/product.biblio.jsp?osti_id=4783132)
- [21] F. D. Becchetti, C. A. Fields, R. S. Raymond, H. C. Bhang, D. Overway, Ghost anomaly in Be 8 studied with Be 9 ( p , d ) at E p = 14.3 and 26.2 MeV, *Physical Review C* 24 (6) (1981) 2401–2408. doi:10.1103/PhysRevC.24.2401.  
URL <https://link.aps.org/doi/10.1103/PhysRevC.24.2401>
- [22] S. Hyldegaard, Beta-decay studies of  $^9\text{Be}$ , Ph.D. thesis, Aarhus University (2010).  
URL [https://wiki.kern.phys.au.dk/Solveig/\\_Hyldegaard.pdf](https://wiki.kern.phys.au.dk/Solveig/_Hyldegaard.pdf)
- [23] V. Meyer, H. Müller, H. Staub, R. Zurmühle, The  $\gamma$ -radiation of the  $^7\text{Li}$  ( p ,  $\gamma$ ) resonance at 441.3 keV, *Nuclear Physics* 27 (2) (1961) 284–293. doi:10.1016/0029-5582(61)90350-9.  
URL <http://linkinghub.elsevier.com/retrieve/pii/0029558261903509>
- [24] A. Boyle, The spin of the 2.9 MeV state of  $^8\text{Be}$ , *Nuclear Physics* 1 (8) (1956) 581–584. doi:10.1016/S0029-5582(56)80078-3.  
URL <https://www.sciencedirect.com/science/article/pii/S0029558256800783>
- [25] I. S. Grant, Radiative Transitions in  $^8\text{Be}$ , *Proceedings of the Physical Society* 76 (5) (1960) 737–744. doi:10.1088/0370-1328/76/5/313.  
URL <http://stacks.iop.org/0370-1328/76/i=5/a=313?key=crossref.196788c71072038943d2fd73df6cdb9d>
- [26] B. Mainsbridge, The angular distributions of the gamma radiation from the  $^7\text{Li}(p,\gamma)^8\text{Be}$  reaction from E p = 200 keV, *Nuclear Physics* 21 (1960) 1–14. doi:10.1016/0029-5582(60)90023-7.  
URL <https://www.sciencedirect.com/science/article/pii/0029558260900237>
- [27] F. Barker, Intermediate coupling shell-model calculations for light nuclei, *Nuclear Physics* 83 (2) (1966) 418–448. doi:10.1016/0029-5582(66)90582-7.  
URL <https://www.sciencedirect.com/science/article/pii/0029558266905827?via=IJDihub>